

# Runx3 negatively regulates Osterix expression in dental pulp cells

Li ZHENG\*, Koichiro IOHARA\*, Masaki ISHIKAWA†, Takeshi INTO\*, Teruko TAKANO-YAMAMOTO‡, Kenji MATSUSHITA\* and Misako NAKASHIMA\*<sup>1</sup>

\*Laboratory of Oral Disease Research, National Institute for Longevity Sciences, National Center for Geriatrics and Gerontology, Aichi 474-8522, Japan, †Department of Endodontology and Operative Dentistry, Division of Oral Rehabilitation, Faculty of Dental Science, Kyushu University, Fukuoka 812-8582, Japan, and ‡Division of Orthodontics and Dentofacial Orthopedics, Graduate School of Dentistry, Tohoku University, Sendai 980-8575, Japan

Osterix, a zinc-finger-containing transcription factor, is required for osteoblast differentiation and bone formation. *Osterix* is also expressed in dental mesenchymal cells of the tooth germ. However, transcriptional regulation by Osterix in tooth development is not clear. Genetic studies in osteogenesis place *Osterix* downstream of Runx2 (Runt-related 2). The expression of *Osterix* in odontoblasts overlaps with Runx3 during terminal differentiation *in vivo*. Runx3 down-regulates *Osterix* expression in mouse DPCs (dental pulp cells). Therefore the regulatory role of Runx3 on *Osterix* expression in tooth development was investigated. Enforced expression of Runx3 down-regulated the activity of the *Osterix* promoter in the human embryonic kidney 293 cell line.

When the Runx3 responsive element on the *Osterix* promoter, located at –713 to –707 bp (site 3, AGTGGTT) relative to the cap site, was mutated, this down-regulation was abrogated. Furthermore, electrophoretic mobility-shift assay and chromatin immunoprecipitation assays in mouse DPCs demonstrated direct functional binding of Runx3 to the *Osterix* promoter. These results demonstrate the transcriptional regulation of *Osterix* expression by Runx3 during differentiation of dental pulp cells into odontoblasts during tooth development.

**Key words:** bone morphogenetic protein 2 (BMP2), dental pulp cell (DPC), Osterix, Runx2, Runx3, tooth development.

## INTRODUCTION

The transcriptional regulation of cell proliferation and differentiation by the Runx (Runt-related) family of DNA-binding transcription factors is critical for both morphogenesis and regeneration. The regulatory function of the Runx family on the promoters and enhancers of target genes, where they associate with co-factors and other DNA-binding transcription factors to modulate gene expression, is well known [1]. The Runx family is composed of three members designated Runx1 (AML1/Cbfa2), Runx2 (AML2/Cbfa1) and Runx3 (AML3/Cbfa3) [2,3]. Although the Runx members share highly conserved DNA-binding domains, they regulate distinct functions [4–7]. Runx1 is involved in the regulation of haematopoiesis [8], Runx2 is essential for bone and tooth development [9–11], and Runx3 is critical for gastric epithelial differentiation, neurogenesis of the dorsal root ganglia and T cell differentiation [8–10,12–16].

Stringent control of gene activation and suppression is required for tooth development. The optimal gene expression during dentin formation is dependent on integration and regulation of signals that govern the commitment of stem/progenitor cells into the pulp cell lineage, and their subsequent proliferation and differentiation into odontoblasts. Runx2 is essential for tooth formation. Molar development is arrested at the late bud stage in Runx2 homozygous mice [11], correlating with the intense expression of Runx2 in the dental mesenchyme during the bud and cap stages [17]. Runx3 is co-expressed in dental papillae at the cap and early bell stages, along with Runx2. Later Runx3 is restricted to the odontoblastic layer at the late bell stage, while Runx2 is no longer detected [17]. Runx proteins might play a pivotal role in governing the control of the physiological response of dental genes.

Osterix, a zinc-finger-containing transcription factor, is required for osteoblast differentiation and bone formation [18]. In *Osterix* null mice, no bone formation occurs, similar to the phenotypes in *Runx2* null mice [9,18]. However, Runx2 is expressed without major alterations in *Osterix* null mice. In contrast, Osterix is not expressed in *Runx2* null mice, demonstrating that Osterix acts downstream of Runx2 [18]. Transcriptional regulation of *Osterix* by Runx2 in cartilage has been suggested recently [19]. In addition, *Osterix* expression has been observed in mesenchymal cells of the tooth germ [18]. The expression of *Osterix* and its transcriptional regulation by Runx proteins during tooth development have not been investigated.

In the present study, we investigated the expression of *Osterix* during tooth development, and demonstrate that *Osterix* is expressed strictly in the odontoblastic layer at the bell and the differentiation stages, overlapping with *Runx3*. Therefore the regulation of the expression of *Osterix* by Runx3 was examined further. Our results demonstrate that Runx3 binds directly to the *Osterix* promoter and down-regulates its expression in DPCs (dental pulp cells).

## EXPERIMENTAL

### Cloning of the *Osterix* promoter

To clone the *Osterix* promoter (nucleotides 66 to 1751; GenBank accession no. DQ229136), genomic DNA was isolated from the tail of an ICR mouse. PCR was performed using two primers: *Osterix* promoter 5′-1, 5′-TCTGTCCCTCAGTCCTGCTT-3′ and *Osterix* promoter 3′-2, 5′-GGGCAAGTTGTTCAGAGCTTC-3′. The approx. 1.7 kbp PCR product was then subcloned into MluI

Abbreviations used: BMP, bone morphogenetic protein; ChIP, chromatin immunoprecipitation; DIG, digoxigenin; DMEM, Dulbecco's modified Eagle's medium; DPC, dental pulp cell; Dspp, dentin sialophosphoprotein; DTT, dithiothreitol; EGFP, enhanced green fluorescent protein; EMSA, electrophoretic mobility-shift assay; FBS, foetal bovine serum; HEK-293, human embryonic kidney 293; KLK4, kallikrein 4; MSCV, murine stem cell virus; P1, postnatal day 1; RT, reverse transcription; Runx, Runt-related.

<sup>1</sup> To whom correspondence should be addressed (email misako@nils.go.jp).

and XhoI digested pGL3-promoter vector (Promega, Madison, WI, U.S.A.), and named pOx1.7-luc. To prepare the MSCV (murine stem cell virus)-EGFP (enhanced green fluorescent protein)-FLAG-Runx3 expression vector, the following primers were used: FLAG-Runx3-5', 5'-GGCAGATCTGCCACCATGGACTACAAGGACGATGACGACAAGGCTTCCAACAGCATCTTTG-3' and Flag-Runx3-3', 5'-ATATGAGCTCTCCCGCGTGGT-3' to generate a Runx3 fragment with FLAG motif at N-terminal. The 300 bp PCR product was cloned in between the BglII and SacI sites in the pSL1180 vector (GE Healthcare, Buckinghamshire, U.K.) and named Flag-Runx3-300 bp-pSL1180. A 1.0 kbp Runx3 fragment was digested with SacI from the MSCV-EGFP-Runx3 plasmid (kindly provided by Dr Taniuchi Ichiro, Laboratory of Transcriptional Regulation, RIKEN Research Centre for Allergy and Immunology, Yokohama, Japan) and subcloned into the FLAG-Runx3-300 bp-pSL1180 vector to give FLAG-Runx3-pSL1180. The N-terminally FLAG-tagged full-length 1.3 kbp Runx3 was digested with BglII from FLAG-Runx3-pSL1180 and subcloned into the MSCV-EGFP vector, named MSCV-EGFP-FLAG-Runx3. The orientation of the inserts was confirmed by sequencing.

### Site-directed mutagenesis

Three putative Runx2-binding sequences at positions -1823 to -1817 bp, -1776 to -1771 bp and -713 to -707 bp relative to the Cap site [19] were mutated using the QuikChange® Site-Directed Mutagenesis Kit (Stratagene, La Jolla, CA, U.S.A.) according to the manufacturer's recommendations. We generated mutants as follows; 5'-AACCACA-3' at -1823/-1817 bp was changed into 5'-GAGCTCA-3', 5'-ACCACT-3' at -1776/-1771 bp was changed into 5'-GCTACT-3' and 5'-AGTGGTT-3' at -713/-707 bp was changed into 5'-ATAGACT-3'. The mutated nucleotides are indicated in bold. Mutations in single, double, and triple motifs were termed M1-M5 (Figure 3B). Incorporation of the mutated substitutions of all the constructs was confirmed by sequencing.

### In situ hybridization

ICR mouse embryos at 15.0 days post coitum, 17.0 days post coitum and P1 (postnatal day 1) were fixed in 4% (w/v) paraformaldehyde at 4°C overnight. *In situ* hybridization was carried out as described previously [20]. The following primers were used to amplify the mouse *Osterix* cDNA: *Osterix*-5'-1, 5'-GGTCCAGCAACACACCTAC-3' and *Osterix*-3'-2, 5'-GGTAGGGA-GCTGGGTAAAGG-3'. The PCR product was ligated into the pBluescript II SK (-) vector (Stratagene). Mouse *Runx3* cDNA was removed from the MSCV-EGFP-Runx3 plasmid by digestion with EcoRI and then subcloned into the pBluescript II SK (-) vector. All inserts were confirmed by sequencing. The following cDNAs were used to generate sense (see Supplementary Figure 1 at <http://www.BiochemJ.org/bj/405/bj4050069add.htm>) and antisense riboprobes using either T3 or T7 RNA polymerase: a 184 bp murine *Osterix* fragment, a 1.2 kb *Runx3* fragment and a 1.2 kb *Bmp2* fragment. *In situ* hybridization was performed as described previously [21].

### Cell culture and transfection studies

Mouse DPCs were isolated from tooth germ at 17.0 days post coitum. Mouse DPCs and HEK-293 (human embryonic kidney 293) cells were maintained in DMEM (Dulbecco's modified Eagle's medium) (Sigma, St. Louis, MO, U.S.A.) supplemented with 100 units/ml penicillin G, 100 µg/ml streptomycin (Invitrogen, Carlsbad, CA, U.S.A.) and 10% (v/v) FBS (foetal bovine

**Table 1 Primers for RT-PCR**

Name	Direction	Sequence	Product size (bp)	Accession number
<i>β</i> -Actin	Forward	5'-AAATCGTGCCTGACATCAA-3'	178	X03765
	Reverse	5'-AAGGAAGGCTGGAAAAGAGC-3'		
Runx3	Forward	5'-GGTTCAACGACCTTCGATTC-3'	180	NM_019732
	Reverse	5'-AGGCCTTGGTCTGGTCTTCT-3'		
Runx2	Forward	5'-CAGACCAGCAGCACTCCATA-3'	178	NM_009820
	Reverse	5'-CAGCGTCAACACCATCATT-3'		
Osterix	Forward	5'-GGTCCAGGCAACACACCTAC-3'	178	AF184902
	Reverse	5'-GGTAGGAGCTGGGTTAAGG-3'		
Dspp	Forward	5'-GGAAGTGCAGCAGAGATGA-3'	199	NM_010080
	Reverse	5'-CAGTGTCCCTGTTCTGTTT-3'		
Enamelysin	Forward	5'-CGACAATGCTGAGAAGTGA-3'	180	NM_013903
	Reverse	5'-CCCTTTCACATCATCCTGG-3'		
Klk4	Forward	5'-TTGCAACAGATCTCATGCTC-3'	228	NM_019928
	Reverse	5'-TGAGGTGGTACACAGGGTCA-3'		

serum; SAFC Biosciences, Lenexa, KS, U.S.A.). Experiments assessing promoter activity by luciferase reporter gene expression were performed as follows. HEK-293 cells ( $1 \times 10^5$ ) were plated in 24-well plates in serum-free DMEM without antibiotics 1 day before use, and transiently transfected with 2 µg of the promoter-luciferase reporter gene plasmids, 3 µg of expression plasmid and 0.2 µg of SV40 (simian virus 40) promoter construct (Promega) as an internal standardized control for transfection efficiency. Transfections were performed using 2 µl/well of Lipofectamine™ 2000 (Invitrogen) following the manufacturer's instructions. The MSCV-EGFP plasmid was also transfected as a control. After 4 h, the medium was replaced with DMEM supplemented with 10% (v/v) FBS and cultured for an additional 44 h. Cells were then lysed, and luciferase activity was determined using a Dual Luciferase Reporter Assay kit as instructed by the manufacturer (Promega). All activities were normalized against the co-transfected internal control plasmid pRL-SV40 (Promega). For over-expression experiments,  $4 \times 10^6$  DPCs were transfected with 8 µg of expression plasmid using an ECM 830 Electroporator (BTX, San Diego, CA, U.S.A.) following the manufacturer's instructions, then plated on to a collagen type I-coated 35-mm-diameter dish (Iwaki, Chiba, Japan). After 4 h, the medium was replaced with DMEM and 10% (v/v) FBS. Cells were harvested at 0, 24 and 48 h after transfection. The cell viability was determined with Trypan Blue soon after transfection, and the efficiency was estimated by fluorescent microscopy 24 h after transfection with the plasmid vector AFP (kindly provided by Dr Hidesato Ogawa, Graduate School of Biological Sciences, Nara Institute of Science and Technology, Japan).

### Real time RT (reverse transcriptase)-PCR analysis

Total RNA was extracted by using Trizol (Invitrogen), and 2 µg of freshly isolated RNA was reverse transcribed with SuperScript II RT (Invitrogen) following the manufacturer's recommendations. The resulting cDNA was then amplified by real time RT-PCR with a Light Cycler-FastStart DNA master SYBR Green I (Roche Diagnostics, Mannheim, Germany). The primers used in the RT-PCR analysis are presented in Table 1.

### Preparation of nuclear extracts

Nuclear extract was isolated as described previously [22]. Briefly, mouse DPCs were washed with 10 ml of PBS, scraped into 1.5 ml of ice-cold PBS, and centrifuged at 100 g for 5 min. The pellet was suspended in 1 ml of PBS and centrifuged again at 660 g

for 15 s. After resuspension in cold buffer A [10 mM Hepes, pH 7.9, 10 mM KCl, 0.1 mM EDTA, 0.1 mM EGTA, 1 mM DTT (dithiothreitol) and 0.5 mM PMSF] on ice for 15 min, the cell membranes were lysed by 0.5 % Nonidet P40 and then centrifuged at 660 g for 30 s. The pelleted nuclei were resuspended in cold buffer C (20 mM Hepes, pH 7.9, 0.4 M NaCl, 1 mM EDTA, 1 mM EGTA, 1 mM DTT and 1 mM PMSF). The nuclear protein was extracted by shaking at 4 °C for 15 min, followed by centrifugation at 15 000 g for 5 min and the supernatant fractions were collected. The protein content of the nuclear extracts was determined using the Bradford method [23].

### EMSA (electrophoretic mobility-shift assay)

Individual oligonucleotides were annealed to equimolar amounts of their complementary strands (wild-type, *Osterix*-gel-WT-5'-1: 5'-CAGATCTCTAATTAGTGGTTTGGGGTTTGTTCCT-TTTC-3' and *Osterix*-gel-WT-3'-2: 5'-GAAAAGGAACAAAC-CCCAAACCACTAATTAGAGATCTG-3'; mutant, *Osterix*-gel-MT-5'-1: 5'-CAGATCTCTAATTATAGACTTGGGGTTTGTTC-CTTTTC-3' and *Osterix*-gel-MT-3'-2: 5'-GAAAAGGAACAA-ACCCCAAGTCTATAATTAGAGATCTG-3') by heating to 95 °C for 5 min and cooling slowly to room temperature (25 °C). DIG (digoxigenin) Gel Shift Kit, 2nd generation (Roche Diagnostics) was used in the EMSA according to the manufacturer's protocol. Briefly, wild-type double-stranded oligonucleotide probes were labelled with DIG-11-ddUTP at the 3'-ends. The labelled probes (20 fmol) were added to 10 µg of nuclear extract in a binding buffer [20 mM Hepes, pH 7.6, 1 mM EDTA, 10 mM (NH<sub>4</sub>)<sub>2</sub>SO<sub>4</sub>, 1 mM DTT, 0.2 % (w/v) Tween 20, 30 mM KCl, 25 ng/µl poly(dI-dC) · (dI-dC), 25 ng/µl poly(dA-dT) · (dA-dT) and 50 ng/µl poly L-lysine] at room temperature for 30 min. For competition experiments, 125-fold unlabelled oligonucleotides were added to the mixture. After incubation, the protein–DNA complexes were separated by native PAGE (6% gels), transferred on to a nylon membrane (Whatman, New Jersey, NJ, U.S.A.) by contact-blotting, and detected by the DIG-detection kit. An anti-Runx3 antibody (Active Motif, Carlsbad, CA, U.S.A.) was used to examine the specificity of the protein–DNA complexes.

### ChIP (chromatin immunoprecipitation) assay

Mouse DPCs were treated for 10 min with 1 % formaldehyde and washed three times with ice-cold PBS. The cells were harvested and centrifuged at 100 g for 5 min. The pellet was suspended in 200 µl of SDS lysis buffer [50 mM Tris/HCl, pH 8.0, 10 mM EDTA, 1 % (w/v) SDS, 1 mM PMSF, 1 µg/ml aprotinin and 1 µg/ml leupeptin] and incubated on ice for 20 min. The sample was sonicated for 7.5 min (high power, on 30 s, off 1 min) using a Bioruptor (Cosmo Bio, Tokyo, Japan) to produce soluble chromatin with an average size of 500 bp. The chromatin sample was then diluted 9-fold in ice-cold ChIP dilution buffer [50 mM Tris/HCl, pH 8.0, 167 mM NaCl, 1.1 % (v/v) Triton X-100, 0.11 % sodium deoxycholate, 1 mM PMSF, 1 µg/ml aprotinin and 1 µg/ml leupeptin]. From the diluted sample, 200 µl was removed as the input fraction and kept at 4 °C. The rest of the sample was pre-cleared for 6 h at 4 °C by incubation with 60 µl of protein G–Sepharose beads pre-blocked with salmon sperm DNA. The beads were removed by centrifugation at 10 000 g for 10 s and the supernatant was collected. Rabbit anti-Runx3 polyclonal antibody (20 µg; Active Motif, Carlsbad, CA, U.S.A.) or 10 µg of goat anti-mouse Runx2 polyclonal antibody (Santa Cruz, CA, U.S.A.) was added and incubated overnight at 4 °C. To collect the immunocomplex, 60 µl of protein G–Sepharose beads pre-blocked with salmon sperm DNA were added to the samples for

3 h at 4 °C. The beads were washed once in each of the following buffers, in order: low salt, high salt and LiCl wash solution, and were then washed twice in TE buffer. The bound protein–DNA immunocomplexes were eluted twice with 200 µl of ChIP direct elution buffer (10 mM Tris/HCl, pH 8.0, 300 mM NaCl, 5 mM EDTA and 0.5 % SDS) and subjected to reverse cross-linking at 65 °C for 6 h. The reverse cross-linked chromatin DNA was further purified by 50 µg/ml proteinase K digestion at 55 °C for 1 h and phenol/chloroform extraction. DNA was then precipitated in ethanol and dissolved in 20 µl of TE buffer. DNA (2 µl) was used for each PCR with primers *Osx*-ChIP-F: 5'-GAGTGTTCG-TCCCAATCC-3' and *Osx*-ChIP-R: 5'-CTGCTACCACCG-AGGCTG-3', yielding a 120 bp product. As a negative control, another 1 × 10<sup>7</sup> mouse DPCs was treated as above, except 20 µg rabbit IgG or 10 µg goat IgG antibodies were used instead of specific antibodies. Input (diluted 1:20) was used as the positive control for PCR.

### Statistics

Statistical analyses were performed using Student's unpaired *t* test. Each experiment was performed at least twice, and the representative data are presented as means ± S.D. for at least three independent replicates.

## RESULTS

### Expression of *Runx3*, *Runx2*, *Osterix* and *Bmp2* during tooth development

In the developing tooth, *Runx3* was detected in the dental papillae at the late cap stage (15.0 days post coitum). *Runx3* was progressively restricted to the odontoblastic layer of tooth germ from the bell stage (17.0 days post coitum) until the differentiation stage, P1 during terminal differentiation of odontoblasts (Figures 1A–1D). In contrast, *Osterix* was first detected in the odontoblastic layer at 17.0 days post coitum, and was more pronounced at P1 and P4 (Figures 1E–1H) and had overlapping expression with *Runx3*. In the odontoblasts, *Bmp2* also was strongly expressed at P1 (Figure 1O), but not *Runx2* (Figure 1K). No positive signal was detected when using sense probes.

### Expression of *Runx3* and *Osterix* during differentiation of the dental pulp cells into odontoblasts *in vitro*

We next determined whether the mouse DPCs have *in vitro* expression patterns of *Runx3* and *Osterix* similar to those observed *in vivo*. RT-PCR was performed to examine gene expression of *Runx3*, *Osterix* and the odontoblast markers *Dspp* (dentin sialoprophosphoprotein), *enamelysin* and *KLK4* (kallikrein 4) in cell culture (Figure 2A). *Dspp* and *KLK4* were first detected clearly on day 21 and *enamelysin* on day 28, showing spontaneous differentiation of the DPCs into odontoblasts. *Runx3* expression was weakly detected on day 1, and increased further on day 21. *Osterix* expression was first detected on day 21 (Figure 2A). These results correlated with the *in vivo* expression during tooth development, suggesting that the DPCs might be useful for the study of the regulation of expression of *Osterix* by Runx3 at the stage before terminal differentiation of odontoblasts.

### Runx3 down-regulates *Osterix* expression in mouse DPCs

To examine whether *Osterix* expression was regulated by Runx3, MSCV-EGFP-Flag-Runx3 was transfected by electroporation into the mouse DPCs. Electroporation, at three square-wave pulses at a frequency of 1 Hz with a pulse length of 99 µs and 1350 V, provided an optimal method for gene transfer *in vitro*. The cell

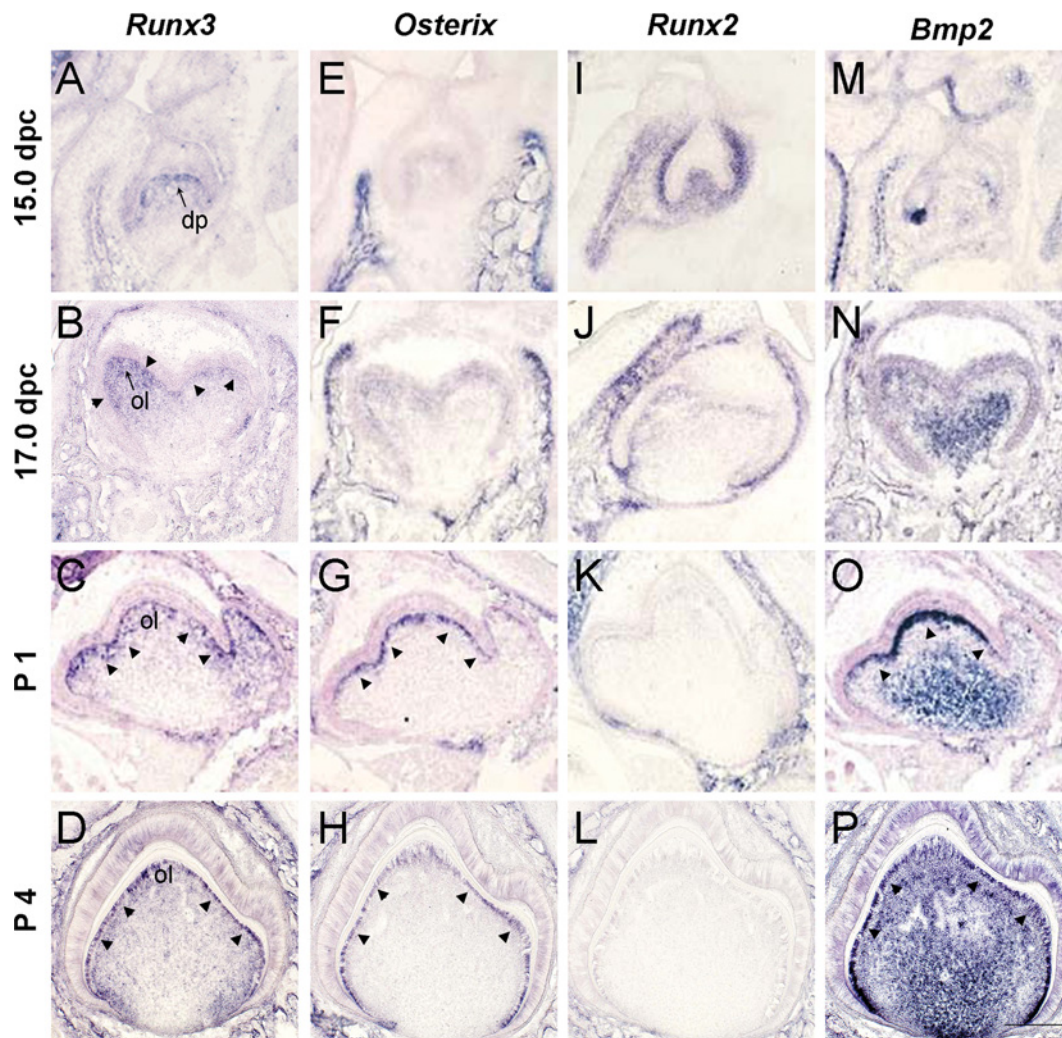


**Figure 1** Expression of *Runx3*, *Osterix*, *Runx2* and *Bmp2* by *in situ* hybridization during tooth development in mouse

(A–D) *Runx3* was progressively restricted to the odontoblastic layer of tooth germ starting from the bell stage (17.0 days post coitum) to the differentiation stage (P1) during terminal differentiation of odontoblasts. (E–H) *Osterix* was first detected weakly in the odontoblastic layer at 17.0 days post coitum, and was a more pronounced at P1, overlapping with *Runx3* expression. (I–L) *Runx2* was not expressed in odontoblast layer after P1. (M–P) *Bmp2* was strongly expressed in the odontoblasts at P1. Arrowheads indicate the positive signals in the odontoblastic layer. dp, dental papillae; ol, odontoblast layer. Scale bar = 200  $\mu$ m.

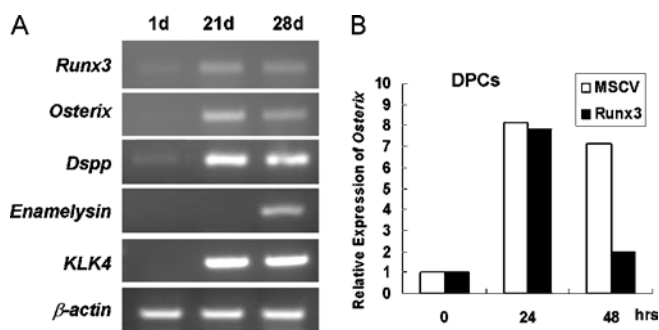


**Figure 2** Down-regulation of *Osterix* expression by *Runx3* in mouse DPCs *in vitro*

(A) mRNA expression levels for *Runx3*, *Osterix*, and for the differentiation markers of odontoblasts, *Dspp*, *enamelysin* and *KLK4* in mouse DPCs in cell culture. (B) *Osterix* expression was down-regulated in mouse DPCs at 48 h after *Runx3* transfection. The experiment was repeated twice with similar results.

viability was nearly 70%, as determined with Trypan Blue staining, and the efficiency was nearly 35%, as estimated by fluorescence microscopy. Real-time RT-PCR showed that the expression of *Runx3* mRNA was enhanced approx. 3-fold in DPCs transfected with MSCV-EGFP-Flag-*Runx3* compared with control DPCs transfected with MSCV-EGFP after 24 h (results not shown). *Runx3* mRNA expression levels, however, were reduced to almost the same level as the control 48 h after transfection. On the other hand, *Osterix* expression was reduced by 25% 48 h after transfection with MSCV-EGFP-Flag-*Runx3* compared with control transfections (Figure 2B). These results suggest that *Runx3* negatively regulates *Osterix* expression in the DPCs.

#### **Runx3 down-regulates the *Osterix* promoter activity in HEK-293 cells**

A recent study has shown that *Runx2* specifically up-regulated *Osterix* promoter activity in C3H10T1/2 and ATDC5 cells, which are mesenchymal cell lines from bone and cartilage respectively

[19]. There has, so far, been no report concerning *Osterix* regulation by Runx3. Runx3 shares highly conserved DNA-binding domains with Runx2. Both the *Runx2* and the *Runx3* promoters have putative Runx-binding sites that are fully conserved in sequence and location [24], therefore cross-regulation between Runx2 and Runx3 might be plausible. To avoid this possible endogenous effect, HEK-293 cells, in which neither Runx2 nor Runx3 are expressed (Figure 3A), were used to examine transcriptional activity induced by Runx3.

Three putative Runx-binding sites were identified at positions –1823 to –1817 bp (site 1, ACCACA), –1776 to –1771 bp (site 2, ACCACT) and –713 to –707 bp (site 3, AGTGGTT) relative to the cap site by computer analysis of the *Osterix* promoter (Figure 3B). A wild-type luciferase reporter plasmid containing all the three putative Runx-binding sites was compared with the *Osterix* promoter containing five different mutations (M1–M5), in which some of the three putative sites were mutated (Figure 3B). Cells in which the wild-type reporter plasmid was co-transfected with Runx3 reduced the *Osterix* promoter activity to approx. 55%. Transfection of the mutant reporters in which site 1 and/or site 2 were mutated resulted in almost the same reduced activity as that of the wild-type promoter. In contrast, in the mutant reporters in which site 3 was mutated (M4 and M5), only a weak repression (approx. 90% activity) was detected (Figure 3B). These results suggest that site 3 is essential for *Osterix* promoter activity. To confirm this, shorter wild-type and mutant plasmids containing only site 3 were used. The *Osterix* promoter activity was significantly reduced in cells transfected with the wild-type construct, whereas the cells transfected with the mutant construct were unaffected (Figure 3C). These results suggest that site 3 is essential for *Osterix* promoter activity.

### Characterization of Runx3 binding to site 3

To determine whether transcriptional repression of *Osterix* is due to direct binding of Runx3 to site 3, EMSAs using nuclear extracts from the mouse DPCs were performed. As shown in Figure 4(A), 38 bp end-labelled oligonucleotide containing the site 3 (–713 to –707 bp) of the *Osterix* promoter formed a DNA–protein complex (Figure 4A, lane 2, arrowhead). The complex was competed out completely by a 125-fold excess of unlabelled wild-type oligonucleotide (Figure 4A, lane 3). An oligonucleotide in which site 3 was mutated did not affect this binding (Figure 4A, lane 4). Furthermore, an anti-Runx3 antibody bound to the DNA–protein complex (Figure 4A, lane 5, arrow), indicating the specificity of the DNA–protein complex. No band could be detected when only nuclear extract was loaded (Figure 4A, lane 6).

Next, we performed ChIP assays to test if Runx3 binds specifically to the putative response element *in vivo*. Using mouse DPCs, proteins were cross-linked on to chromatin and immunoprecipitated with an anti-Runx3 antibody. The presence of the *Osterix* promoter DNA was detected by PCR using primers flanking site 3 (–713 to –707 bp) (Figure 4B), indicating that Runx3 binds to site 3 of *Osterix* promoter both specifically and functionally. The use of an anti-Runx2 antibody resulted in a similar result (Figure 4B), suggesting that both Runx3 and Runx2 are able to bind site 3 *in vivo*.

### DISCUSSION

During a systematic *in situ* hybridization study of tooth development, *Osterix* mRNA was first detected in terminally differentiating odontoblasts and showed co-localization with *Runx3*, suggesting a potential role for both genes in odontoblast differentiation. Runx3 overexpression resulted in down-regulation

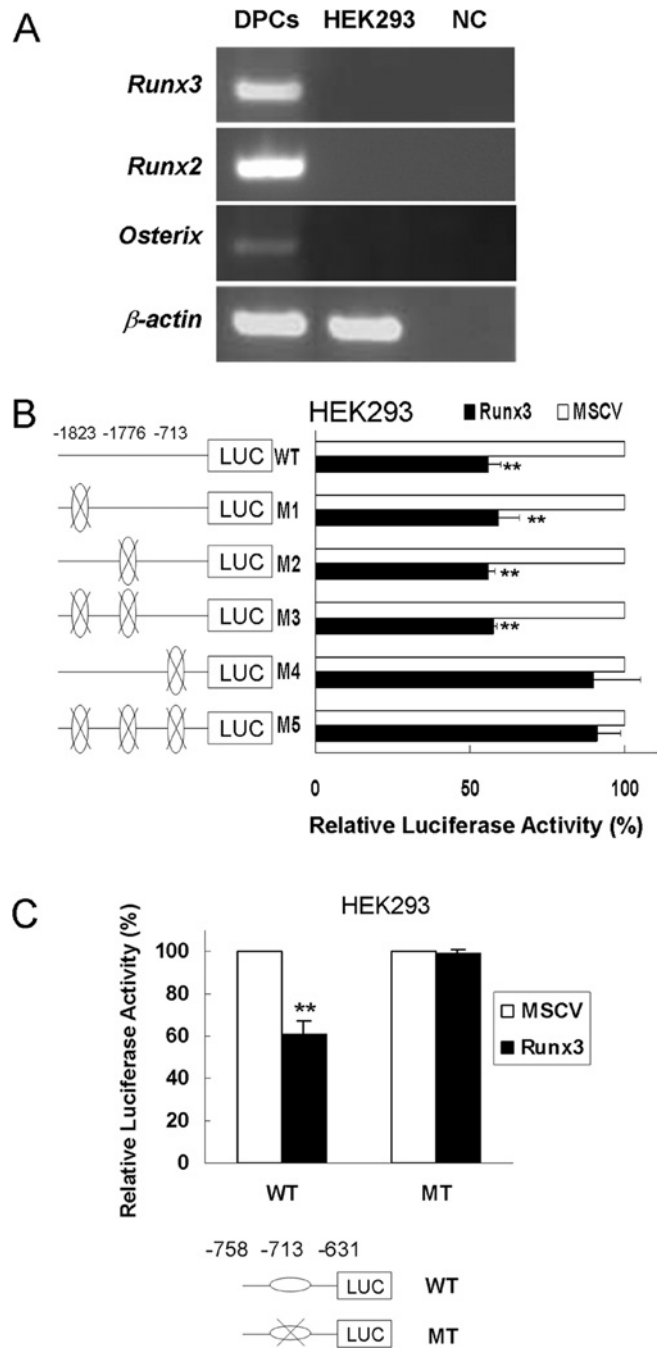


**Figure 3** Down-regulation of *Osterix* promoter activity by Runx3 in HEK-293 cells

(A) Determination of endogenous expression levels of *Runx3*, *Runx2* and *Osterix* in mouse DPCs and HEK-293 cells. (B) Wild-type (WT) and mutant (MT) *Osterix* promoter plasmids were analysed 48 h after co-transfection with MSCV-EGFP-Flag-Runx3 into HEK293 cells. (C) Shortened wild-type (WT) or mutant (MT) *Osterix* promoter plasmids containing only site 3 (–713 to –707) were co-transfected with MSCV-EGFP-Flag-Runx3 into HEK-293 cells. The activities were determined after 48 h and normalized against the co-transfected internal control plasmid (pRL-SV40). The values represent means  $\pm$  S.D. for four individual samples. The experiment was repeated twice with similar results. \*\*,  $P < 0.01$  compared with the empty MSCV plasmid. NC, negative control.

of *Osterix* in the mouse DPCs. This suggests that *Osterix* might be a downstream target of *Runx3* in tooth development. *Osterix* null mice [18] have a similar phenotype to the *Runx2* null mice [9,10], in which both intramembranous and endochondral bone are not

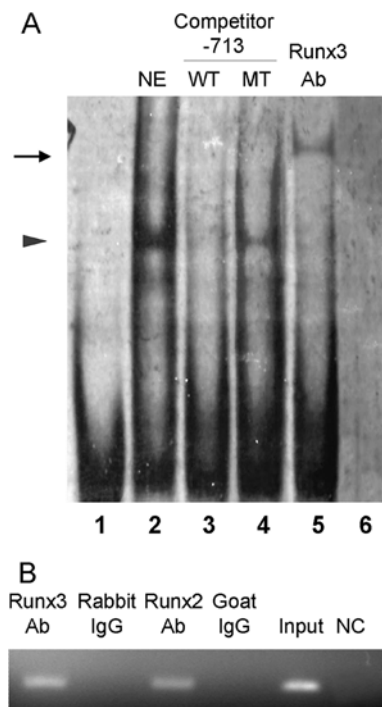


**Figure 4** Characterization of Runx3 binding to the *Osterix* promoter by EMSA and ChIP assay

(A) Interaction of nuclear extract (NE) of mouse DPCs with *Osterix* promoter –713 to –707 bp sequence (site 3) in EMSA. The arrowhead indicates the retarded protein–DNA complexes. The arrow indicates the super-shift band in the reaction with the addition of an anti-Runx3 antibody (lane 5). Lane 1 shows a binding reaction with no protein. Lane 2 is a control reaction with no competing oligonucleotides. Lanes 3 and 4 represent competition reactions with wild-type (WT) or mutated (MT) unlabelled oligonucleotides. Lane 6, nuclear extract only. (B) ChIP assays were performed to investigate whether both Runx3 and Runx2 could bind to the *Osterix* promoter *in vivo*. A 120-bp band could be detected by PCR in both anti-Runx3 and anti-Runx2 antibody treated samples, but not in anti-rabbit or anti-goat IgG treated samples. Ab, antibody; NC, negative control.

formed due to the lack of osteoblast differentiation. Whereas *Osterix* is not expressed in the *Runx2* null mutants, *Runx2* expression is not changed in the *Osterix* null mutants [18]. These genetic studies have placed *Osterix* downstream of *Runx2* [18]. The precise regulatory role of Runx2 in *Osterix* expression is not clear. A recent study has shown that a 737 bp fragment of the *Osterix* promoter is up-regulated upon *Runx2* overexpression in ATDC5 chondrogenitor cells, and the function of the 737 bp fragment was confirmed by site-directed mutagenesis experiments [19]. Furthermore, this functional binding site is conserved among mouse, rat and human, showing conservation of the DNA-binding site [19]. However, no information is available on the regulation of *Osterix* expression by Runx3. Therefore, we have performed transient co-transfection, EMSAs and ChIP assays to investigate the relationship between Runx3 and *Osterix* in DPCs. Structural dissection of the proximal promoter of the *Osterix* gene revealed the presence of three putative Runx-binding sites. Only site 3 (–713 to –707 bp) of the identified sites was preferentially and functionally occupied by Runx3. The disruption of site 3 leads to increased *Osterix* promoter activity in HEK-293 cells, in which both Runx2 and Runx3 are not expressed endogenously. These results indicate that *Osterix* expression is negatively regulated by Runx3. Furthermore, our EMSAs and ChIP assays confirmed that Runx3 directly down-regulates *Osterix* expression in DPCs prior to terminal differentiation into odontoblasts. It is noteworthy that Runx3 negatively regulates *CD36* expression in myeloid cells

[25] and suppresses gastric epithelial cell growth [26], implying a general role for Runx3 in transcriptional repression.

The distinct roles of Runx2 and Runx3 in odontoblast differentiation are not clear. Previous research indicated that tooth development was disrupted in the cap/early bell stages in the *Runx2* null mice and no overt differentiation of odontoblasts was observed [11,27]. There was no conspicuous phenotype in teeth of *Runx3* null mice [17]. In *Runx2* null mice, *Runx3* expression was enhanced dramatically in the mesenchyme of upper molars, and they differentiated into odontoblasts [27]. Our EMSAs and ChIP assays have shown that not only Runx2, but also Runx3 binds to site 3 of the *Osterix* promoter. *Runx3* overexpression resulted in down-regulation of *Osterix* in DPCs. The *Osterix* promoter activity was down-regulated by *Runx3* transfection in HEK-293 cells. These results suggest that *Osterix* expression is co-operatively regulated by Runx2 and that Runx3 is sharing the same binding site on the *Osterix* promoter. Thus, Runx3 might co-operate with Runx2 to regulate *Osterix* expression during odontoblast differentiation. The role of *Osterix* in tooth development is not clear. In skeletal development, Runx2, Runx3 and *Osterix* play pivotal roles in osteoblast differentiation and hypertrophic chondrocyte maturation [28,29]. *Osterix* may play a role in segregation of osteoblast and chondrocyte lineages [29,30]. *Runx2* and *Runx3* are co-expressed in the early stages of tooth development. There is overlapping expression of *Osterix* with *Runx3*, but not with *Runx2* in terminal differentiation of odontoblasts. Therefore *Osterix* may play a role in lineage commitment of odontoblasts in tooth development. The diverse transcriptional outcomes of Runx activity are dependent on context [1]. The Runx family members act as organizing factors on the promoters of target genes, where they associate with co-activators and other DNA-binding transcription factors, including Smads [1]. Repression of *Osterix* by Runx3 in DPCs is an example of context-dependent regulation of lineage commitment. Thus, there might be co-operative interactions among BMPs, Smads, Runx2 and Runx3 in the regulation of *Osterix* expression during DPC differentiation into odontoblasts.

We thank Professor A. Akamine (Department of Dental Science, Faculty of Dental Science, Kyushu University, Fukuoka, Japan) for his help. This work was supported by a Grant-in-Aid for Scientific Research from the Ministry of Education, Science, Sports and Culture, Japan, #17390509 and #18-06588.

## REFERENCES

- Durst, K. L. and Hiebert, S. W. (2004) Role of RUNX family members in transcriptional repression and gene silencing. *Oncogene* **23**, 4220–4224
- Ito, Y. (2004) Oncogenic potential of the RUNX gene family: 'overview'. *Oncogene* **23**, 4198–4208
- van Wijnen, A. J., Stein, G. S., Gergen, J. P., Groner, Y., Hiebert, S. W., Ito, Y., Liu, P., Neil, J. C., Ohki, M. and Speck, N. (2004) Nomenclature for Runt-related (RUNX) proteins. *Oncogene* **23**, 4209–4210
- Bangsow, C., Rubins, N., Glusman, G., Bernstein, Y., Negreanu, V., Goldenberg, D., Lotem, J., Ben-Asher, E., Lancet, D., Levanon, D. and Groner, Y. (2001) The RUNX3 gene—sequence, structure and regulated expression. *Gene* **279**, 221–232
- Levanon, D., Glusman, G., Bangsow, T., Ben-Asher, E., Male, D. A., Avidan, N., Bangsow, C., Hattori, M., Taylor, T. D., Taudien, S. et al. (2001) Architecture and anatomy of the genomic locus encoding the human leukemia-associated transcription factor RUNX1/AML1. *Gene* **262**, 23–33
- Ogawa, E., Maruyama, M., Kagoshima, H., Inuzuka, M., Lu, J., Satake, M., Shigesada, K. and Ito, Y. (1993) PEBP2/PEA2 represents a family of transcription factors homologous to the products of the *Drosophila runt* gene and the human *AML1* gene. *Proc. Natl. Acad. Sci. U.S.A.* **90**, 6859–6863
- Thirunavukkarasu, K., Mahajan, M., McLaren, K. W., Stifani, S. and Karsenty, G. (1998) Two domains unique to osteoblast-specific transcription factor *Osf2/Cbfa1* contribute to its transactivation function and its inability to heterodimerize with *Cbfb*. *Mol. Cell. Biol.* **18**, 4197–4208

- 8 Komori, T. (2005) Regulation of skeletal development by the Runx family of transcription factors. *J. Cell. Biochem.* **95**, 445–453
- 9 Komori, T., Yagi, H., Nomura, S., Yamaguchi, A., Sasaki, K., Deguchi, K., Shimizu, Y., Bronson, R. T., Gao, Y. H., Inada, M. et al. (1997) Targeted disruption of *Cbfa1* results in complete lack of bone formation owing to maturational arrest of osteoblasts. *Cell* **89**, 755–764
- 10 Otto, F., Thornell, A. P., Crompton, T., Denzel, A., Gilmour, K. C., Rosewell, I. R., Stamp, G. W., Beddington, R. S., Mundlos, S., Olsen, B. R. et al. (1997) *Cbfa1*, a candidate gene for cleidocranial dysplasia syndrome, is essential for osteoblast differentiation and bone development. *Cell* **89**, 765–771
- 11 D'Souza, R. N., Aberg, T., Gaikwad, J., Cavender, A., Owen, M., Karsenty, G. and Thesleff, I. (1999) *Cbfa1* is required for epithelial-mesenchymal interactions regulating tooth development in mice. *Development* **126**, 2911–2920
- 12 Ducy, P., Zhang, R., Geoffroy, V., Ridall, A. L. and Karsenty, G. (1997) *Osf2/Cbfa1*: a transcriptional activator of osteoblast differentiation. *Cell* **89**, 747–754
- 13 Mundlos, S., Otto, F., Mundlos, C., Mulliken, J. B., Aylsworth, A. S., Albright, S., Lindhout, D., Cole, W. G., Henn, W., Knoll, J. H. et al. (1997) Mutations involving the transcription factor CBFA1 cause cleidocranial dysplasia. *Cell* **89**, 773–779
- 14 Li, Q. L., Ito, K., Sakakura, C., Fukamachi, H., Inoue, K., Chi, X. Z., Lee, K. Y., Nomura, S., Lee, C. W., Han, S. B. et al. (2002) Causal relationship between the loss of RUNX3 expression and gastric cancer. *Cell* **109**, 113–124
- 15 Levanon, D., Bettoun, D., Harris-Cerruti, C., Woolf, E., Negreanu, V., Eilam, R., Bernstein, Y., Goldenberg, D., Xiao, C., Fliegau, M. et al. (2002) The Runx3 transcription factor regulates development and survival of TrkC dorsal root ganglia neurons. *EMBO J.* **21**, 3454–3463
- 16 Brenner, O., Levanon, D., Negreanu, V., Golubkov, O., Fainaru, O., Woolf, E. and Groner, Y. (2004) Loss of Runx3 function in leukocytes is associated with spontaneously developed colitis and gastric mucosal hyperplasia. *Proc. Natl. Acad. Sci. U.S.A.* **101**, 16016–16021
- 17 Yamashiro, T., Aberg, T., Levanon, D., Groner, Y. and Thesleff, I. (2002) Expression of Runx1, -2 and -3 during tooth, palate and craniofacial bone development. *Mech. Dev.* **119** (Suppl. 1), S107–S110
- 18 Nakashima, K., Zhou, X., Kunkel, G., Zhang, Z., Deng, J. M., Behringer, R. R. and de Crombrughe, B. (2002) The novel zinc finger-containing transcription factor Osterix is required for osteoblast differentiation and bone formation. *Cell* **108**, 17–29
- 19 Nishio, Y., Dong, Y., Paris, M., O'Keefe, R. J., Schwarz, E. M. and Drissi, H. (2006) Runx2-mediated regulation of the zinc finger Osterix/Sp7 gene. *Gene* **372**, 62–70
- 20 Platt, K. A., Michaud, J. and Joyner, A. L. (1997) Expression of the mouse *Gli* and *Ptc* genes is adjacent to embryonic sources of hedgehog signals suggesting a conservation of pathways between flies and mice. *Mech. Dev.* **62**, 121–135
- 21 Iohara, K., Zheng, L., Ito, M., Tomokiyo, A., Matsushita, K. and Nakashima, M. (2006) Side population cells isolated from porcine dental pulp tissue with self-renewal and multipotency for dentinogenesis, chondrogenesis, adipogenesis, and neurogenesis. *Stem Cells* **24**, 2493–2503
- 22 Schreiber, E., Matthias, P., Muller, M. M. and Schaffner, W. (1989) Rapid detection of octamer binding proteins with 'mini-extracts', prepared from a small number of cells. *Nucleic Acids Res.* **17**, 6419
- 23 Bradford, M. M. (1976) A rapid and sensitive method for the quantitation of microgram quantities of protein utilizing the principle of protein-dye binding. *Anal. Biochem.* **72**, 248–254
- 24 Drissi, H., Luc, Q., Shakoobi, R., Chuva De Sousa Lopes, S., Choi, J. Y., Terry, A., Hu, M., Jones, S., Neil, J. C., Lian, J. B. et al. (2000) Transcriptional autoregulation of the bone related CBFA1/RUNX2 gene. *J. Cell Physiol.* **184**, 341–350
- 25 Puig-Kroger, A., Dominguez-Soto, A., Martinez-Munoz, L., Serrano-Gomez, D., Lopez-Bravo, M., Sierra-Filardi, E., Fernandez-Ruiz, E., Ruiz-Velasco, N., Ardavin, C., Groner, Y. et al. (2006) RUNX3 negatively regulates CD36 expression in myeloid cell lines. *J. Immunol.* **177**, 2107–2114
- 26 Chi, X. Z., Yang, J. O., Lee, K. Y., Ito, K., Sakakura, C., Li, Q. L., Kim, H. R., Cha, E. J., Lee, Y. H., Kaneda, A. et al. (2005) RUNX3 suppresses gastric epithelial cell growth by inducing p21<sup>WAF1/Cip1</sup> expression in cooperation with transforming growth factor  $\beta$ -activated SMAD. *Mol. Cell Biol.* **25**, 8097–8107
- 27 Aberg, T., Cavender, A., Gaikwad, J. S., Bronckers, A. L., Wang, X., Waltimo-Siren, J., Thesleff, I. and D'Souza, R. N. (2004) Phenotypic changes in dentition of Runx2 homozygote-null mutant mice. *J. Histochem. Cytochem.* **52**, 131–139
- 28 Yoshida, C. A. and Komori, T. (2005) Role of Runx proteins in chondrogenesis. *Crit. Rev. Eukaryot. Gene Expr.* **15**, 243–254
- 29 Komori, T. (2006) Regulation of osteoblast differentiation by transcription factors. *J. Cell. Biochem.* **99**, 1233–1239
- 30 Nakashima, K. and de Crombrughe, B. (2003) Transcriptional mechanisms in osteoblast differentiation and bone formation. *Trends Genet.* **19**, 458–466